Cosmic Magnetic Fields and their Role in High Energy Astrophysics

Robi Banerjee[1], *Günter Sigl*[2]

[1]Hamburger Sternwarte, Universität Hamburg, Germany
[2]II. Institut für Theoretische Physik, Universität Hamburg, Germany

DOI: http://dx.doi.org/10.3204/PUBDB-2018-00782/C9

Magnetic fields play an important role in many astrophysical and cosmological situations. The evolution of primordial seed fields crucially depends on the amount of helicity and the properties of the velocity field. On the other hand, magnetic fields can serve as an agent for possible signatures of dark matter in the form of annihilating weakly interacting massive particles, through induced synchrotron radiation of charged annihilation products, and for a possible mixing of axion-like particles and other light states with photons in scenarios beyond the Standard Model. In the context of project C9 of the SFB 676 we investigated both the seeding and evolution of magnetic fields and their effects on other processes.

1 Chiral magnetic effect

One possible effect that was increasingly considered in recent years as a possible contribution to seed magnetic fields is the so-called chiral magnetic effect. This effect can transform an initially present chiral asymmetry between left-chiral and right-chiral electrons and positrons into a helical magnetic field the sign of whose helicity is opposite to the sign of the difference of left-chiral and right-chiral lepton number. The helical fields initially grow exponentially on length scales larger than a critical scale indirectly proportional to the absolute value of the chiral asymmetry which is why it is also known as chiral magnetic instability. It is actually very similar to the classical dynamo, where the role of the chiral asymmetry is played by the helicity of the turbulent eddies. At the same time the chiral asymmetry is reduced until some approximate equipartition between the magnetic field energy and the energy associated with the chiral asymmetry is reached, at which point the magnetic field strength saturates and, at later times is damped by resistivity. The chiral asymmetry necessary for chiral magnetic effect can be produced, for example, by the electroweak interaction which breaks the chiral symmetry. This can play a role both in the early Universe, in particular around the electroweak phase transition, and in hot dense nuclear matter where left-chiral electrons and positrons through charged current interactions can turn into neutrinos which leave the star due to their weak interactions, whereas right-chiral electrons and positrons are only subject to neutral current induced scattering. The chiral magnetic effect will be discussed more quantitatively in the report to project C10 where we will also briefly cover its possible role in the electroweak phase transition. Here we restrict ourselves to a brief summary of the possible role of the chiral magnetic effect in hot neutron stars, based on our publication Ref. [1].

When discussing the chiral magnetic effect one usually assumes approximate equilibrium and

characterises the left- and right-chiral leptons by a chemical potential μ_L and μ_R, respectively. In strict thermal equilibrium and if the lepton mass is non-zero, one would have $\mu_L = mu_R$. However, in the presence of a non-vanishing production rate R_w of a chiral asymmetry one can treat the left- and right-chiral as approximately decoupled and at temperature T one gets

$$\frac{|\mu_5|}{T} \simeq \frac{R_w}{R_f}\,, \tag{1}$$

where $\mu_5 = (\mu_L - \mu_R)/2$ and R_f is the spin-flip rate which is of order $(m_e/T)^2$ times the scattering rate. In hot nuclear matter R_w is governed by URCA interactions and scales roughly as T^4, whereas R_f is only logarithmically dependent on temperature. As a result, $|\mu_5|/T$ is strongly temperature dependent and reaches values of order 10^{-3} for $T \simeq 50\,\mathrm{MeV}$, which are temperatures typical for the formation stage of hot neutron stars following a core collapse supernova. The magnetic fields that could be induced by the chiral magnetic instability reaches about 10^{15} Gauss for such temperatures.

2 Cosmic-ray propagation

The public CRPropa simulation tool for propagation of high energy cosmic rays, $\gamma-$rays and neutrinos in a structured Universe including magnetic fields that was developed partly within project C8 and is described in more detail in the corresponding section, was further extended within project C9 [2]. In this context it was applied to simulate the impact of cosmic large scale magnetic fields on high energy cosmic radiation. To extend the applicability to lower energies, where cosmic rays tend to diffuse and a direct simulation of trajectories becomes inefficient, CRPropa was extended to solve transport equations with stochastic differential equations [3]. The coupling to new models of the extragalactic magnetic field based on large scale structure simulations including magnetic fields was the subject of Ref. [4, 5]. The diffusive mode of extragalactic cosmic ray propagation was investigated in Ref. [6]. It was found that below an energy $E \simeq Z\,\mathrm{EeV}$ the fluxes from cosmological sources tend to be suppressed due to a "magnetic horizon". Finally, the recent dipolar anisotropy of ultra-high energy extragalactic cosmic rays above 8×10^{18} eV [7] was interpreted in the context of one dominating nearby source [8]. It was found that a discrete source with a flux corresponding to about 3% of the total flux and a deflection angle $\sim 50^\circ$ at $8 \times 10^{18}\,\mathrm{eV}$ can reproduce the observed dipole as well as limits on the dipole and higher multipoles at higher and lower energies. Interestingly, for a coherence length of $\simeq 100\,\mathrm{kpc}$ this would require an extragalactic magnetic field strength of several nanoGauss. The CRPropa package was also used to clarify the role of the Liouville theorem in the influence of propagation in magnetic fields on ultra-high energy cosmic rays [9].

Cosmic rays at much smaller energies, of the order of 10 MeV kinetic energy, could be accelerated already shortly after the first objects, in particular the first supernovae, formed in the early Universe, starting at redshift $z \simeq 20$. It is not very well known how efficient this process may have been, but in principle it can contribute to heating the neutral intergalactic medium, in addition to contributions from X-rays and possible dark matter (DM) annihilation, before it was significantly re-ionized. We showed in Ref. [10] that such cosmic rays contribute negligibly to re-ionization, but may rise the temperature of the intergalactic medium by between 10 and 200 Kelvin by redshift $z = 10$. Whether this early heating is rather uniform or tends to cluster around the first cosmic ray sources strongly depends on the structure of the magnetic fields present between $z \simeq 20$ and $z \simeq 10$ in which these cosmic rays diffuse. They could, for example,

efficiently confined around their sources if magnetic fields are significantly enhanced by plasma streaming instabilities. These effects can considerably influence the properties of predicted HI 21 cm emission characteristics which is expected to be probed in much detail by future radio surveys with instruments such as LOFAR and the SKA. Heating of the intergalactic medium by energy deposition by early cosmic rays may also influence constraints on DM annihilation and decay based on observations of 21 cm emission. It is also interesting to note in this context that very recently, observations by the Experiment to Detect the Global Epoch of Reionization Signature (EDGES) indicate an absorption profile around 78 MHz, corresponding to the 21 cm line redshifted by $z \simeq 17$, that is about a factor 2 stronger than expected [11]. This suggests that either background radiation temperature was hotter than expected or the temperature of the intergalactic gas around redshift $z \sim 17$ that is much lower than expected. Such and other observations anticipated in the future may thus also constrain the effect of cosmic rays on the intergalactic medium, in particular the cosmic ray production efficiency and the structure of the magnetic fields in which they diffuse.

3 WIMP DM constraints from synchrotron annihilation

WIMP DM annihilation into charged leptons can be constrained through their synchrotron radiation. This signal is also influenced by the diffusion of these charged leptons in the magnetic fields present in the objects where DM annihilation is occurring. Interesting targets are objects that are radio-quiet but at the same time are expected to be dominated by DM. One type of objects are high velocity clouds in the Milky Way, in particular the so-called Smith cloud. There are indications that the Smith cloud has crossed the Galactic plane several times and, in order to not have been disintegrated by tidal forces, should be dominated by DM. In Ref. [12] we analytically modelled the synchrotron emission by first computing the Syrovatskii solution for electrons and positrons produced with a rate given by a radially symmetric DM annihilation profile and an assumed annihilation cross section and branching ratio into electrons and positrons and subsequently diffusing in magnetic fields characterised by an energy dependent spatially constant diffusion coefficient and appropriate continuous energy losses. Based on the resulting radial electron/positron distribution the synchrotron spectrum was computed in a given magnetic field of a few microGauss assumed to be constant. Comparison with sensitivities of radio instruments such as LOFAR, expressed in terms of flux densities or brightness temperature, the lead to constraints on the annihilation cross sections into electrons/positrons as a function of DM mass. Interestingly, for radio frequencies at a few tens of MHz, these constraints can reach below the standard relic thermal cross section $\langle\sigma_{\rm th}\rangle \simeq 3\times10^{-26}\,{\rm cm}^3/{\rm s}$ by factors up to ~ 100 for DM masses $> 100\,{\rm GeV}$ and down to $\simeq 1\,{\rm GeV}$. These studies were subsequently extended to dwarf spheroidal galaxies and galaxy clusters in the context of a masters thesis [13]. Figure 1 shows an example for the sensitivities that can be reached for the dwarf spheroidal Triangulum II.

4 Signatures of ALP conversion into photons

In extensions of the Standard Model involving axion-like particles (ALPs) often a coupling between two photons, represented by the field strength tensor $F_{\mu\nu}$ and its dual $\tilde{F}_{\mu\nu}$, and the

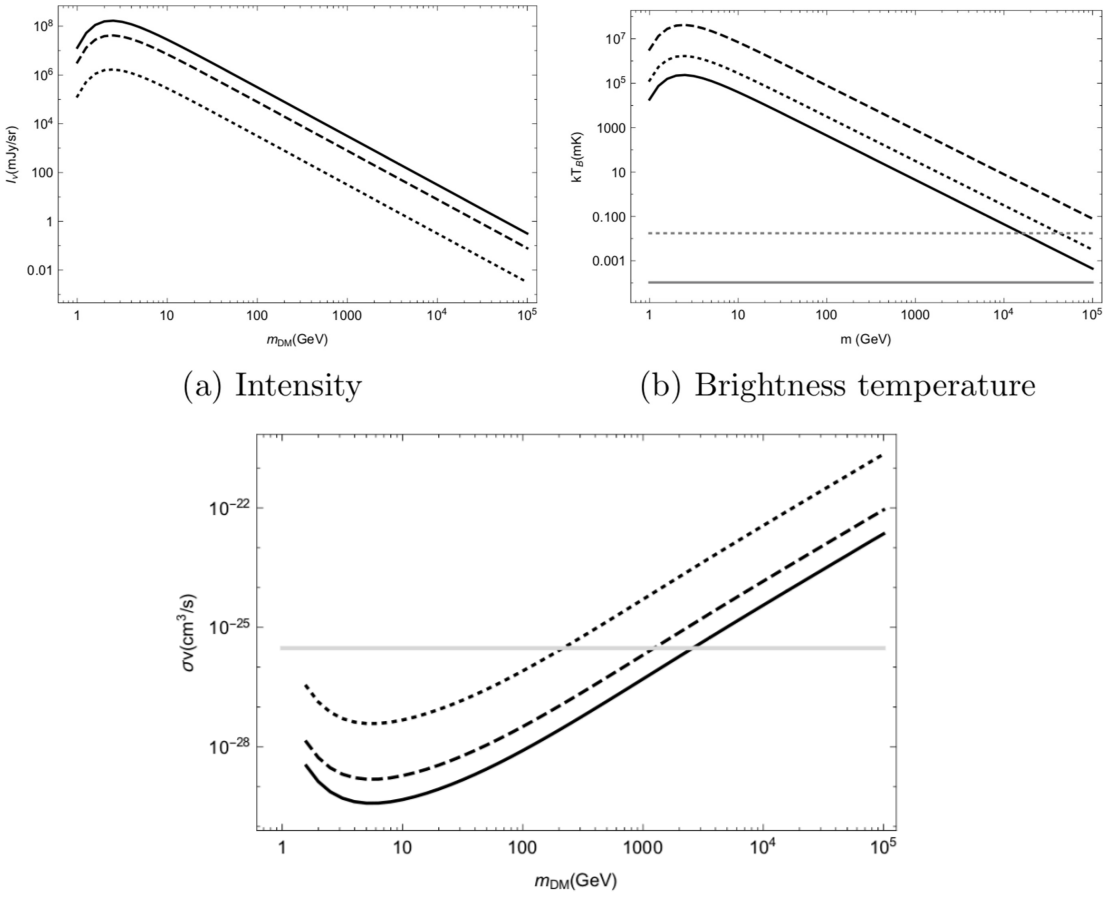

(a) Intensity (b) Brightness temperature

Figure 1: Upper panels: Expected intensity in milliJansky per beam and brightness temperature in milliKelvin for DM self-annihilation into e^+e^- as function of DM mass for the dwarf spheroidal Triangulum II. The different lines indicate uncertainties related to the size of the diffusive halo. Horizontal gray solid line indicates the LOFAR sensitivity for a beamsize of 20×20, the gray dotted line indicates the sensitivity for SKA. Lower panel: Resulting constraints on the annihilation cross section into electrons and positrons as function of DM mass. Horizontal gray line marks the annihilation cross section required for thermal relic cold DM to reproduce the observationally inferred DM abundance. Figure adopted from Ref. [13].

ALP field a of the form

$$\frac{\alpha_{\rm em}}{8\pi}\frac{C_{a\gamma}}{f_a}\, a\, F_{\mu\nu}\tilde{F}^{\mu\nu} = \frac{g_{a\gamma}}{4}\, a\, F_{\mu\nu}\tilde{F}^{\mu\nu} \tag{2}$$

occurs, where $\alpha_{\rm em} = e^2/(4\pi\epsilon_0)$ is the fine structure constant, f_a is a Peccei-Quinn type energy scale, $C_{a\gamma}$ is a model-dependent dimensionless number and $g_{a\gamma} \equiv \alpha_{\rm em} C_{a\gamma}/(2\pi f_a)$ is the effective ALP-photon coupling which is an inverse energy. In the presence of an external electromagnetic field, in particular a magnetic field, this can lead to photon-ALP conversion, also known as Primakoff effect, and can be used to probe the existence of ALPs in contexts rang-

ing from experimental setups, such as light shining through a wall experiments where photons are converted to ALPs which travel through a wall opaque to photons, and are reconverted to photons, or haloscopes where ALPs constitute (part of) DM and are converted to photons, to distortions of the spectra of natural photon sources such as astrophysical $\gamma-$ray sources or the cosmic microwave background (CMB). The conversion efficiency generally depends on the spatial structure, and possibly the time-dependence, of the magnetic field. We will here focus on so-called astrophysical haloscopes where cold DM ALPs are converted to radio lines in magnetised astrophysical objects [14] and distortions of the CMB spectrum through mixing with ALPs in the magnetic fields within galaxy clusters [15].

One can show that in a static magnetic field with isotropic power spectrum per logarithmic wavenumber interval $\rho_m(k,\mathbf{r})$ ALPs convert non-resonantly to a photon line at frequency $\omega_\gamma = m_a$ centered on the ALP mass m_a with fractional width $\Delta = \Delta\omega_\gamma/\omega_\gamma \lesssim 10^{-3}$ and the total flux density of a source at distance d can be written as

$$S \simeq \frac{\pi}{4d^2}\frac{g_{a\gamma}^2}{m_a^2}\frac{1}{\Delta}\int d^3\mathbf{r}\rho_a(\mathbf{r})\rho_m(m_a,\mathbf{r}) \simeq \frac{\pi}{4d^2}\frac{g_{a\gamma}^2}{m_a^2}\frac{1}{\Delta}M_a\rho_m(m_a)\,, \tag{3}$$

where $\rho_a(\mathbf{r})$ is the local ALP mass density and in the last step we have assumed the ALP and magnetic field densities to be roughly constant with M_a the total ALP mass within the object. Inserting characteristic numbers this gives [14]

$$S \simeq 2.8\times10^{-11}\,\left(g_{a\gamma}10^{14}\,\mathrm{GeV}\right)^2\left(\frac{m_a}{\mu\mathrm{eV}}\right)^{-2}\left(\frac{10^{-3}}{\Delta}\right)\left(\frac{M_a}{10^{-10}\,M_\odot}\right)\left(\frac{d}{\mathrm{kpc}}\right)^{-2}\left(\frac{B}{\mathrm{G}}\right)^2 f(m_a)\,\mathrm{Jy}\,, \tag{4}$$

where $f(k)$ is the fraction of the total magnetic field energy density in a logarithmic wavenumber interval centered at k. However, the total flux density cannot exceed

$$S_{\max} \simeq \frac{\rho_a}{m_a}\frac{v_a}{\Delta}\left(\frac{r_s}{d}\right)^2 \simeq 10^{-10}\left(\frac{m_a}{\mu\mathrm{eV}}\right)^{-1}\left(\frac{r_s}{10^6\,\mathrm{cm}}\right)^2\left(\frac{d}{\mathrm{kpc}}\right)^{-2}\mathrm{Jy}\,, \tag{5}$$

which would correspond to complete conversion of all ALPs impinging on the object of radius r_s with velocity v_a. Resonant ALP DM to photon conversion, which is also limited by Eq. (5), was recently considered for neutron stars in Refs. [16,17].

The conversion of CMB photons to ALPs and the resulting distortion of the CMB is strongly constrained by the very precisely measured CMB spectrum. Viewing the CMB through galaxy clusters is in particular interesting in this case, for one because the magnetic field strength in galaxy clusters is known to be a few micro Gauss, and also because the distortion of the CMB by the hot plasma in these clusters, known as the thermal Sunyaev–Zeldovich (tSZ) effect, is well measured in terms of the distortion parameter y. The idea is then that photon-ALP conversion and the tSZ effect lead to very different distortion spectra, as shown in Fig. 2. Since no deviations from the expected tSZ distortions have been observed, this allows to put constraints on the coupling $g_{a\gamma}$. In particular, for the mass range 2×10^{-14} eV $\lesssim m_a \lesssim 3\times10^{-12}$ eV we found that a future PRISM-like experiment would allow limits up to $g_{a\gamma} \lesssim \mathcal{O}(10^{-13}\ \mathrm{GeV}^{-1})$, 1.5 orders of magnitude stronger than the currently strongest limits in this mass range.

A thesis on the role of magnetic fields in various astrophysical and cosmological contexts has been published in Ref. [18]. Furthermore, magnetic fields also constitute energy-momentum and thus can source gravitational waves. The strength of the resulting gravitational fields was investigated in the context of a master thesis [19].

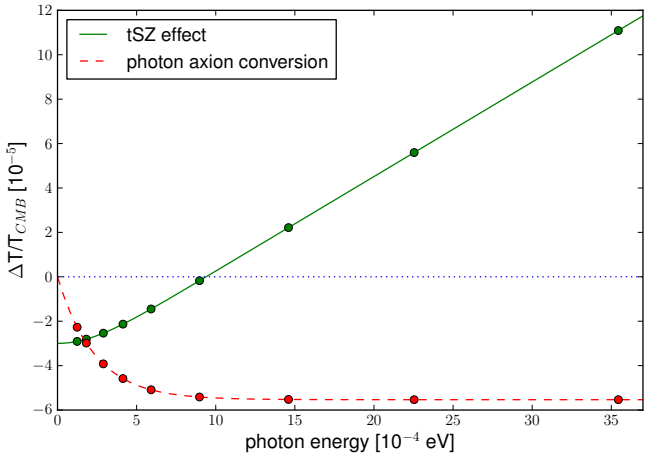

Figure 2: Comparison of the spectral profile of the tSZ effect (with y = 10^{-5}) and the photon-axion conversion. The horizontal axis shows the photon energy, the vertical axis shows the relative distortion of the effective CMB temperature, $\Delta T/T_{\rm CMB}$ in units of 10^{-5}. For this plot, the parameters $g_{a\gamma} = 5 \times 10^{-13}$ GeV^{-1} for the ALP-photon coupling, galaxy cluster magnetic field strength $B = 2$ μG, galaxy cluster size $R = 0.5$ Mpc, ALP mass $m_a = 10^{-13}$ eV were used. Different values for these parameters change the normalization of the effect but not its dependence on the photon frequency. The filled circles refer to the centers of the frequency bands of the *Planck*-mission. Figure taken from Ref. [15].

5 Magnetic field amplification by the small-scale dynamo in the early Universe

In [20] we showed that the Universe is already strongly magnetized at very early epochs during cosmic evolution. Our calculations are based on the efficient amplification of weak magnetic seed fields, which are unavoidably present in the early Universe, by the turbulent small-scale dynamo. We identify two mechanisms for the generation of turbulence in the radiation dominated epoch where velocity fluctuations are produced by the primordial density perturbation and by possible first-order phase transitions at the electroweak or QCD scales. We show that all the necessities for the small-scale dynamo to work are fulfilled. Hence, this mechanism, operating due to primordial density perturbations, guarantees fields with comoving field strength $B_0 \sim 10^{-6}\varepsilon^{1/2}$ nG on scales up to $\lambda_c \sim 0.1$ pc, where ε is the saturation efficiency. The amplification of magnetic seed fields could be even larger if there are first-order phase transitions in the early Universe. Where, on scales up to $\lambda_c \sim 100$ pc, the comoving field strength due to this mechanism will be $B_0 \sim 10^{-3}\varepsilon^{1/2}$ nG at the present time. Such fields, albeit on small scales, can play an important role in structure formation and could provide an explanation to the apparently observed magnetic fields in the voids of the large-scale structure

The discrepancy between theoretically generated and observed magnetic fields in the Universe needs explaining. The galactic dynamo can be a very effective mechanism at producing the μG fields observed in spiral galaxies [21]. However, strong fields in young galaxies, clusters and superclusters of galaxies and in the intergalactic medium require further explanation [22–26].

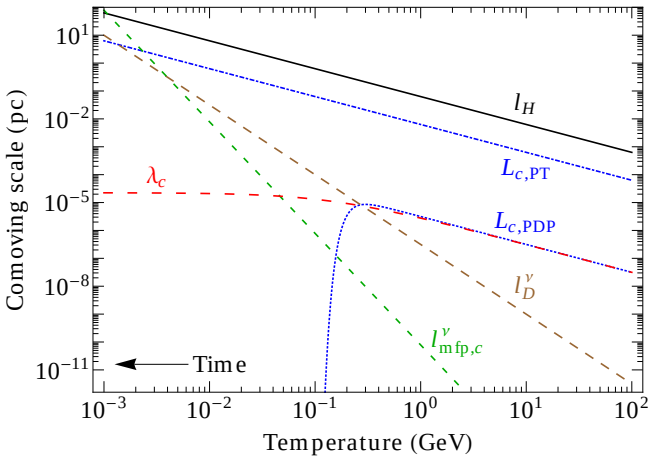

Figure 3: This figure shows the evolution of relevant comoving scales from the EW scale $T_{\mathrm{EW}} \sim 100$ GeV to the time of neutrino decoupling at $T_{\mathrm{dec}} \simeq 2.6$ MeV. In this early epoch the neutrinos generate the plasma viscosity. The QCD phase transition occurs at around $T_{\mathrm{QCD}} \simeq 200$ MeV. Here, $l_H = 1/aH$ is the Hubble scale (solid, black), $l^\nu_{\mathrm{mfp},c}$ is the neutrino mean-free-path (dashed, green) and l^ν_D is the damping scale due to neutrino diffusion (dashed, brown). For turbulence generated by the primordial density perturbation (PDP) and first-order phase transitions (PT), the largest stirring scales $L_c = v_L^{\mathrm{rms}}/aH$. Although the turbulent motions from PDP become completely damped below $T \simeq 0.2$ GeV, the magnetic field gets *frozen-in* with integral scale λ_c (dashed, red). Reprinted figure with permission from Ref. [20]. Copyright (2014) by the American Physical Society.

As noted in a number of numerical and analytical works, the rapid amplification of magnetic seed fields can occur due to the turbulent motions of the conducting plasma. This small-scale dynamo (SSD) mechanism is believed to play a crucial role in the formation of large magnetic fields in a number of astronomical settings, from stars to galaxies and the intergalactic medium [27–31]. For these settings, the turbulent motions arise from gravitational collapse, accretion and supernovae explosions. Hence, the SSD mechanism can be highly effective at magnetizing structures in the early Universe. However, the large field strengths apparently observed in the voids of the large-scale structure [26] still require an explanation.

Magnetic seed fields will almost certainly be generated at some level in the early Universe through a variety of mechanisms. Such mechanisms include inflation [32], phase transitions [33] and the Harrison mechanism through the generation of vorticity [34]. The SSD mechanism for the amplification of such seed fields could play an important role for the explanation of the observed large magnetic fields throughout the Universe. In this paper we have demonstrated that the conditions necessary for such turbulent amplification arise in the radiation dominated Universe before the onset of structure formation. We have shown that significant turbulence is generated in this early epoch by at least two mechanisms; velocity perturbations generated by the primordial density perturbation and bubble collisions in first-order phase transitions.

Turbulent plasma motions arise inevitably from perturbations of the gravitational potential. The continuous production of velocity perturbations upon horizon entry of primordial density modes, act as a continuous forcing of the fluid on the largest scales. Therefore, in regimes of

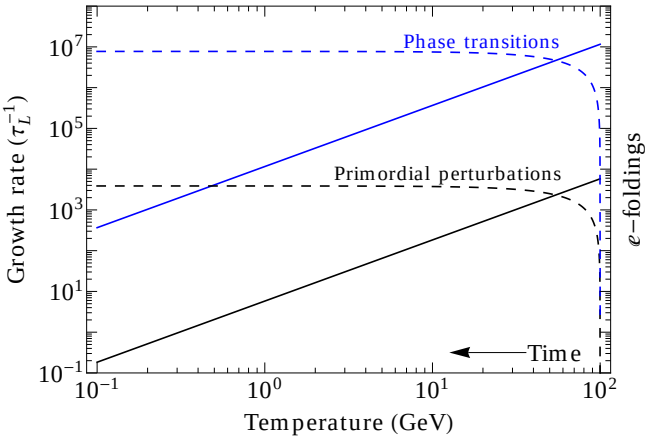

Figure 4: This figure shows the SSD growth rate Γ (solid) and number of e-foldings $N = \int \Gamma(t)dt$ (dashed) from the time of the EW scale $T_{\rm EW} \sim 100$ GeV to the QCD scale $T_{\rm QCD} \simeq 200$ MeV. Recall that the magnetic seed field is amplified as $B_{\rm rms} \propto \exp(\Gamma t)$. The growth rate in units of the eddy-turnover-time where Kolmogorov turbulence $\vartheta = 1/3$ is assumed. The growth rate and the number of e-foldings for turbulence generated by the primordial density perturbation and first-order phase transitions are shown in (black) and (blue) respectively. Reprinted figure with permission from Ref. [20]. Copyright (2014) by the American Physical Society.

large Reynolds numbers, a state of stationary fully developed turbulence is expected. Turbulent flow can be triggered, for example, by thermal fluctuations on very small scales [35]. Turbulence can also be injected into the plasma by bubble collisions during first-order phase transitions. Although the kinetic energy injection occurs only for the duration of the phase transition, we argue, following Refs. [36, 37], that a state of fully developed turbulence is also expected from this mechanism.

Let us first consider the turbulence generated by the primordial density perturbations (PDP). From Fig. 3 we can see that for $T \gtrsim 0.2$ GeV the stirring scale $L_{c,\rm PDP}$ (the lower blue dotted line in the figure) is larger than the damping scale l_D^{ν}. Hence, the velocity perturbations are not damped and one can use density fluctuation-induced rms velocities.

Once fully developed turbulence is established, the Kazantsev model of the SSD mechanism can be used to estimate the magnetic field growth rate. We have demonstrated that the Prandtl numbers are very large in the regime considered. Thus, the results from the Kazantsev theory for $P_m \gg 1$ are applicable. The analytical work shows that the magnetic field growth rate depends on the kinetic Reynolds numbers [38, 39], which are very large in our case. We have shown that, for both models of turbulence, the amplification is strong enough for small magnetic seed fields to reach a saturated state. The saturated state is given by the approximate equipartition between magnetic and kinetic energy $E_{\rm M}/E_{\rm kin} \approx \varepsilon$, where the parameter ε characterizes the efficiency of the mechanism. In Fig. 4 we show the magnetic field growth rate Γ, where $B_{\rm rms} \propto \exp(\Gamma t)$, which is determined from the Kazantsev model of the SSD mechanism. The growth rate depends on the type of turbulence, applicable on the inertial range $l_{\rm diss} < l < L$, for Kolmogorov and Burgers type turbulence respectively. Here, we assume that the turbulence is of Kolmogorov type, which is relevant for the subsonic velocity fluctuations determined in this paper. Now, since Γ varies in time, it will be useful to consider the number of e-foldings

given by $N \equiv \int \Gamma(t) \mathrm{d}t$.

We note that numerical studies at Prandtl numbers $P_m \approx 2$ indicate that the SSD mechanism is more efficient for rotational modes, where the saturation efficiency ε is close to unity [40]. Whereas the saturation level is lower for compressive modes $\varepsilon \sim 10^{-3}$–10^{-4} [40]. However, further numerical work is required to establish the saturation level for larger Prandtl numbers and smaller Mach numbers relevant to our settings. We also note that, although only longitudinal velocity modes are generated by first-order primordial density perturbations, rotational modes are generated at second order in cosmological perturbations [41–45]. Also, there is no reason not to expect rotational modes generated by first-order phase transitions. In any case, since the Reynolds numbers are so large, nonlinear interactions can play a role leading to a state of fully developed turbulence with both rotational and longitudinal modes. In particular, we expect that, below the integral scale, Kolmogorov type turbulence is established. But we stress that the SSD mechanism works independently of the type of turbulence [38, 39, 46]. Indeed, even purely irrotational turbulence can still drive a small-scale dynamo [38–40] . Hence, the efficient amplification of magnetic fields seems unavoidable, leading to a strongly magnetized early Universe prior to structure formation.

For the two mechanisms of turbulence investigated in this paper, we calculated the saturated field strengths and their subsequent evolution up to the present day. We note that although turbulence is completely erased in viscous and free-streaming regimes, magnetic fields are overdamped and can survive to the present day. Therefore, the most important epochs of evolution are due to free turbulent decay. This turbulent MHD effect decreases the field strength and increases the coherence length in nonhelical fields [47, 48]. From the turbulence generated by the primordial density perturbation we found $B_0^{\rm rms} \sim 10^{-6}\varepsilon^{1/2}$ nG on scales $\lambda_c \sim 10^{-1}$ pc. Unfortunately, even for a high efficiency factor $\varepsilon \sim 1$, these fields are too weak on too short scales to explain the Fermi observations of TeV Blazars [26]. From the turbulence generated by first-order phase transitions, we found $B_0^{\rm rms} \sim (10^{-6}$–$10^{-3})\varepsilon^{1/2}$ nG on scales $\lambda_c \sim (10^{-1}$–$10^{2})$ pc. Such fields are strong enough to explain the apparent observations of intergalactic magnetic fields suggested by the Fermi results [26]. Thus, in this paper we have demonstrated that the conditions are right for the efficient amplification of magnetic fields via the small-scale dynamo. The mechanism generates large field strengths, albeit on very small scales, which could explain observations of magnetic fields in the voids of the large-scale structure and have an impact on early structure formation.

6 CMB spectral distortions from the decay of causally generated magnetic fields

In [49] we improved previous calculations of the CMB spectral distortions due to the decay of primordial magnetic fields. Our studies are focused on causally generated magnetic fields at the electroweak and QCD phase transitions. We also consider the decay of helical magnetic fields. We show that the decay of non-helical magnetic fields generated at either the electroweak or QCD scale produce μ and y-type distortions below 10^{-8} which are probably not detectable by a future PIXIE-like experiment. We show that magnetic fields generated at the electroweak scale must have a helicity fraction $f_* > 10^{-4}$ in order to produce detectable μ-type distortions. Hence a positive detection coming from the decay of magnetic fields would rule out non-helical primordial magnetic fields and provide a lower bound on the magnetic helicity.

Magnetic fields generated in the very early Universe decay in the radiation dominated epoch

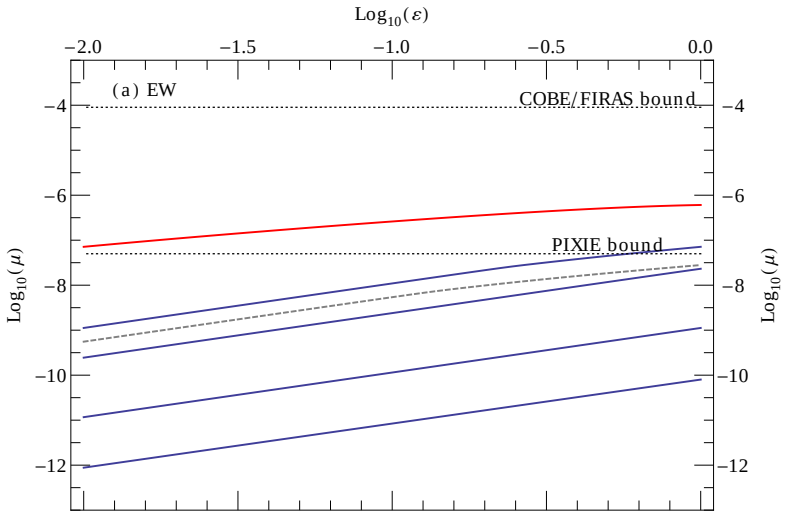

Figure 5: Here we show the μ-type distortion generated due to the decay of magnetic energy initially generated at the EW scale. We plot the spectral distortion μ vs ε, where $\varepsilon \equiv \tilde{\rho}_{B,*}/\rho_{\gamma,0} \approx 1$ corresponds to an initial field strength $\tilde{B}_{\lambda,*} \simeq 3 \times 10^{-6}$ G. The (solid, blue) lines from top to bottom correspond to initial helicity fractions $f_* = \{10^{-3}, 10^{-4}, 10^{-6}, < 10^{-14}\}$. The maximally helical case $f_* = 1$ (solid, red) is also shown. Reprinted figure with permission from Ref. [49]. Copyright (2015) by the American Physical Society.

due to turbulent MHD effects. The decaying magnetic fields inject energy into the primordial plasma which can lead to μ-type and y-type distortions to the CMB black body spectrum. The current COBE/FIRAS limits on these spectral distortions are very tight $|\mu| < 9 \times 10^{-5}$ and $y \lesssim 1.5 \times 10^{-5}$ [50]. However there is the exciting possibility of a new PIXIE-like experiment which could place much stronger upper limits of $|\mu| < 5 \times 10^{-8}$ and $y \lesssim 10^{-8}$ if no detection is made [51]. Any prediction for spectral distortions above the PIXIE limits is what we call detectable.

In this work we consider the evolution of helical and non-helical magnetic fields generated by some causal process in the early Universe. We calculate the spectral distortions using the decays laws of Refs. [47, 52, 53]. We find that causally generated non-helical magnetic fields, with an initial helicity fraction less than $\sim 10^{-14}$, generated at the EW phase transition will not produce any detectable CMB μ-type (see Fig. 5) or y-type (see Fig. 6) spectral distortions. This remains true even if the inverse transfer effect for non-helical fields seen in Refs. [54, 55] is considered. Hence, to produce observable spectral distortions from the decay of magnetic fields generated at the EW phase transition, a non-negligible helical component is required.

Here we note that, if the inverse transfer effect for non-helical fields is applicable [54, 55], it looks possible to generate small amounts of detectable distortions from magnetic fields generated at the QCD phase transition. We also note that magnetogenesis at the QCD phase transition is disfavoured compared to magnetogenesis at the EW phase transition. Under early Universe conditions with very small chemical potentials the QCD phase transition is a smooth transition [56] whereas the EW phase transition could be first-order in certain Standard Model extensions [57].

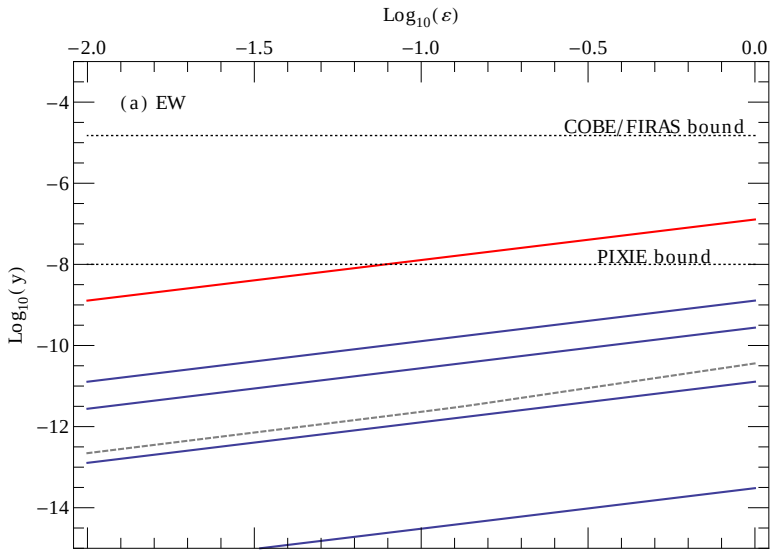

Figure 6: Here we show the y-type distortion produced due to the decay of magnetic energy initially generated at the EW scale. We plot the spectral distortion y vs ε, where $\varepsilon \equiv \tilde{\rho}_{B,*}/\rho_{\gamma,0} \approx 1$ corresponds to an initial field strength of $\tilde{B}_{\lambda,*} \simeq 3 \times 10^{-6}$ G. The (solid, blue) lines from top to bottom correspond to initial helicity fractions $f_* = \{10^{-3}, 10^{-4}, 10^{-6}, < 10^{-14}\}$ and $f_* = \{10^{-1}, 10^{-4}, 10^{-6}, < 10^{-14}\}$ respectively. The maximally helical case $f_* = 1$ (solid, red) is also shown. The final field strength B_0 and coherence length λ_B that would be observed today, i.e. after MHD turbulent decay. We also show (dashed, gray lines) the results from non-helical magnetic fields with an inverse transfer of energy. Reprinted figure with permission from Ref. [49]. Copyright (2015) by the American Physical Society.

The conservation of magnetic helicity in the early Universe leads to an inverse cascade of energy and the slowing down of magnetic decay for fully helical fields. This means that, at the time when CMB spectral distortions can be generated, the magnetic field amplitude is relatively large compared to the non-helical case. This can lead to the generation of larger spectral distortions. If CMB spectral distortions are observed by some new PIXIE-like experiment, then it is likely that magnetic helicity plays an important role. However, there is a degeneracy in the parameter space, since different parameter sets can give the same spectral distortions signal. For example, fields generated at the QCD phase transition with smaller $\varepsilon \equiv \tilde{\rho}_{B,*}/\rho_{\gamma,0}$ and/or helicity can produce the same μ-type distortions as fields generated at the EW phase transition but with larger ε and/or helicity. However, if a μ-type distortion is detected by a PIXIE-like experiment, it would rule out non-helical magnetic fields produced at either the EW or QCD phase transition. A positive detection would give us a lower bound on the primordial magnetic helicity. The lower bound would be somewhere of the order $f_* \gtrsim (10^{-4}$–$10^{-3})$. This is much greater than the primordial magnetic helicity generated in the simplest models of EW baryogenesis [58] where $f_* \sim 10^{-24}$ assuming $B_{\lambda,*} = B^{\rm max}_{\lambda,*}$ and $\lambda_{B,*} = \lambda_{\rm EW}$ [59].

The effect of helical and non-helical magnetic fields in the voids on the propagation of electromagnetic cascades from high energy TeV $\gamma-$ray sources has been investigated in Ref. [60].

In this context it is also interesting to mention the recent tentative observations of large scale helical magnetic fields from γ-ray observations [61]. Such studies have seen some evidence, albeit rather weak, of fully helical fields of strength 10^{-14} G on scales of 10 Mpc. If such fields originated from a time before the μ-era, then it is possible that such observations would be accompanied by a detectable signal for a PIXIE-like experiment. The combination of such two observations would be compelling evidence for large scale helical magnetic fields. We also note that the CMB distortions anisotropies (see e.g. Refs. [62, 63]), albeit potentially very hard to detect, could give interesting signals due to the large helicity of the magnetic fields. Unique signatures in the spatial correlations are expected due to the helical nature of the magnetic fields.

7 Extragalactic magnetic fields unlikely generated at the electroweak phase transition

In the letter [64] we show that magnetic fields generated at the electroweak phase transition are most likely too weak to explain the void magnetic fields apparently observed today unless they have considerable helicity. We show that, in the simplest estimates, the helicity naturally produced in conjunction with the baryon asymmetry is too small to explain observations, which require a helicity fraction at least of order 10^{-14}–10^{-10} depending on the void fields constraint used. Therefore new mechanisms to generate primordial helicity are required if magnetic fields generated during the electroweak phase transition should explain the extragalactic fields.

First-order phase transitions can generate magnetic fields in the early Universe. Under early Universe conditions with very small chemical potentials the QCDPT is a smooth transition [56] whereas the EWPT could be first-order in certain Standard Model (SM) extensions [57]. Inflationary magnetogenesis [32], which is also beyond the SM, is another popular mechanism to explain void magnetic fields. Hence, the apparent observations of void fields from γ-ray observations seem to be a signature of physics beyond the SM or of new mechanisms which excite magnetic helicity (see Sec. 1 and Refs. [65, 66]). If the constraints on void fields prove to be conclusive, then it is likely that magnetic helicity must play an important role. Here we show that magnetic fields generated at the EWPT must have significantly more helicity than that produced by electroweak baryogenesis in order to explain the extragalactic magnetic fields. To reach this conclusion we have assumed the magnetic decay laws of [47, 52, 53] and considered the simplest magnetic helicity estimates of [58] (see Fig. 7). Our assumptions on the decay rates could be challenged due to new results of [54, 55].

8 Nonhelical turbulence and the inverse transfer of energy: A parameter study

In [67] we explore the phenomenon of an *inverse transfer* of energy from large to small scales in decaying magnetohydrodynamical turbulence. For this investigation we mainly employ the *Pencil-Code* performing a parameter study, where we vary the Prandtl number, the kinetic viscosity and the initial spectrum. We find that in order to get a decay which exhibits this *inverse transfer*, large Reynolds numbers ($\mathcal{O} \sim 10^3$) are needed and low Prandtl numbers of the order unity $Pr = 1$ are preferred. Compared to *helical* MHD turbulence, though, the *inverse*

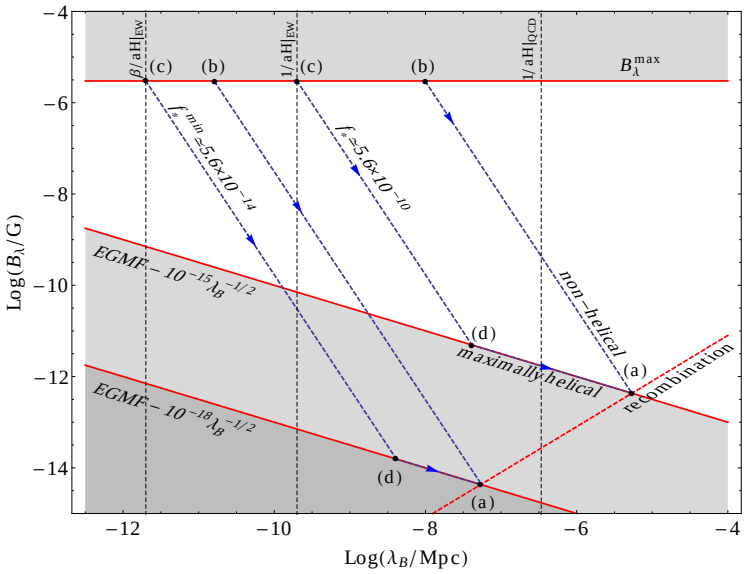

Figure 7: In the greyed out regions, constraints on present day magnetic fields are shown from Fermi observations of γ-ray sources and an upper bound set from energy considerations. Fields generated in the radiation era evolve to the line labelled "recombination". The evolutionary tracks from magnetogenesis until recombination are marked by dashed lines and depend on the helicity fraction f_*. The minimum field configuration at recombination to explain the void fields is marked by point (a). If there is zero helicity, the field configuration at megnetogenesis is marked by point (b). With non-zero helicity the initial field configuration can be reduced e.g point (c), where the field becomes maximally helical at point (d). Figure reprinted from Ref. [64]. © 2016 IOP Publishing Ltd and Sissa Medialab srl.

transfer is much less efficient in transferring magnetic energy to larger scales than the well-known effect of the *inverse cascade*. Hence, applying the *inverse transfer* to the magnetic field evolution in the Early Universe, we question whether the *nonhelical* inverse transfer is effective enough to explain the observed void magnetic fields if a magneto-genesis scenario during the electroweak phase transition is assumed.

Our presented parameter study is based on high-resolution numerical simulations of decaying MHD turbulence. We explored a wide range of numerical parameters and initial conditions in order to find a pattern at which the *inverse transfer* of magnetic energy from small scales to large scales takes place for nonhelical magnetic fields.

Our most prominent finding is the surprising dependency on the Prandtl number: Larger Prandtl numbers lead to a less efficient *inverse transfer* of magnetic energy and might be fully suppressed at Prandtl numbers larger than 10^3. This raises the question whether one can apply the effect of the *inverse transfer* of energy to the evolution of magnetic fields in the early Universe. There, one expects large Prandtl numbers of $\mathrm{Pr} \sim 10^8 (T/\mathrm{keV})^{-3/2}$ [68]. For instance, considering a causally generated field, it will decay according to $E \sim t^{-10/7}$ in the case of suppressed inverse transfer. It will decay as $E \sim t^{-1}$, however, if the inverse transfer is efficient. This results in a many orders of magnitudes weaker field in the former case.

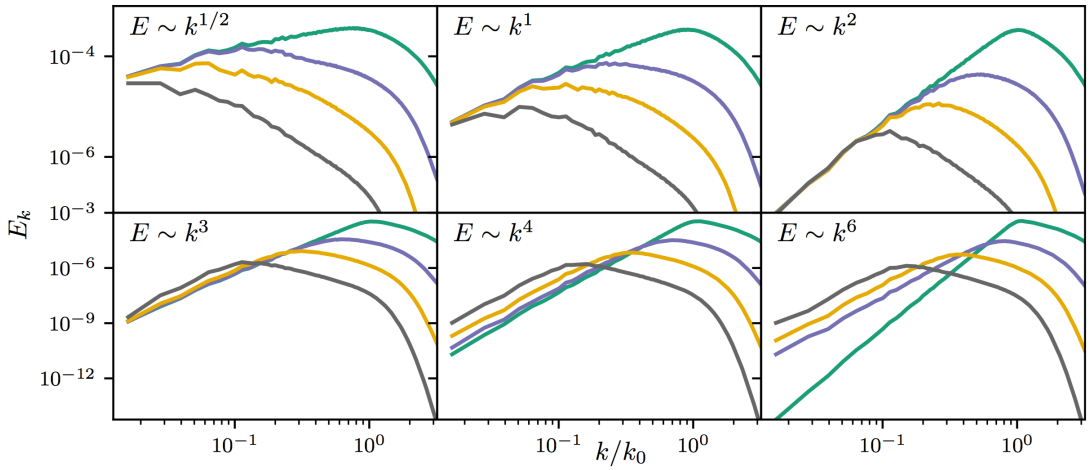

Figure 8: Magnetic power spectra of runs with different spectral indices n. The inverse transfer of energy can only be observed if there is a steep initial spectrum with $n \geq 3$. If an initial spectrum steeper than k^4 is given it will flatten to a *causal* spectrum. Reprinted figure with permission from Ref. [67]. Copyright (2017) by the American Physical Society.

Therefore, it is questionable whether EW phase transition generated fields could be significant enough today to account for the assumed fields in the voids of galaxies (see [64] and [54]).

Furthermore, the efficiency of the *inverse transfer* depends on the Reynolds number. Here, the Reynolds number has to be sufficiently large to observe the effect. With our Pencil-Code simulations we find a critical Reynolds number of $\mathrm{Re} = 500$ for a Prandtl number of $\mathrm{Pr} = 1$.

Another very interesting result of our study is that for shallow and moderately steep slopes of the magnetic power spectrum $n \leq 2$ the effect of the *inverse transfer* is not present. Again, this dependence on n is qualitatively different than the *inverse cascade* of helical fields, which is independent of the spectral index n (see Fig. 8). An $n = 2$ case could be expected from an average over a stochastic distribution of magnetic dipoles [69], and a field with $n = 3/2$ will be generated by the small scale dynamo [70].

Although we find numerical evidence for the effect of non-helical *inverse transfer*, the physics behind this mechanism is yet to be determined. One option could be the enhancement of the magnetic field on large scales by back reactions of velocity fluctuations where the kinetic power spectrum can exceed the magnetic one on scales above the correlation length. Nevertheless, our simulations do not indicate that this mechanism could persist throughout the entire decay phase. See also [55]. Additionally, Brandenburg et al [55] suspect an effect of two-dimensional structure of the turbulence. In two dimensions the square of the vector potential $\langle \mathbf{A}^2 \rangle$ is conserved [71] and could serve as an explanation to the non-helical *inverse transfer*, similar to the conserved helicity in three dimensions. But, $\langle \mathbf{A}^2 \rangle$ varies by at least 80% throughout the simulation time. This is not a lot compared to the magnetic energy which changes by three orders of magnitude during its decay. On the other hand, the helicity in the maximally helical run changes only by a few percent. Nevertheless, the conservation of $\langle \mathbf{A}^2 \rangle$ is not expected in three dimensions and it is not clear why a two-dimensional turbulent structure should develop (depending on the Prandtl number and initial spectral index).

Another way of explaining the inverse transfer is the assumption of a self-similar evolution of the decaying MHD turbulence. Using rescaled MHD variables, Olesen [72] and [73] constructed such a self-similar scenario of decaying MHD turbulence. Although the rescaling of the MHD variables is generally not restricted to a specific choice of the rescaling function, an *inverse transfer* can only be explained by a very specific one where the viscosity is not rescaled, i.e. $\nu \to l^0\nu$ and l is the scale function. First of all, there is no physical reasoning for this (unmotivated) choice and furthermore the rescaling of variables should not impact the physical result. The specific self-similar solution resulting in the *inverse transfer* does not give further insight to this problem. We thus conclude that while there is numerical evidence from our simulations that the non-helical *inverse transfer* of energy can be present, a satisfying physical explanation is still missing.

9 Improved treatment of magnetic heating across the cosmological recombination era

The origin of magnetic fields in the Universe poses many open questions. In [74] we study the evolution of primordial magnetic fields PMF, generated by some early-universe mechanism, across the cosmological recombination epoch, one of the clearly anticipated stages in their evolution. The main goal is to obtain an understanding of the relevant dissipation processes with particular focus on the transition between photon drag-dominated evolution in the pre-recombination era ($z \gtrsim 10^3$) to turbulent decay at later times ($z \lesssim 10^3$). We carry out a suite of numerical MHD simulations studying the dependence of the effective heating rates on the magnetic field strength and spectral index. Our analysis shows that in the drag-dominated phase no real heating of the matter is produced but that the dissipated energy sources small-scale anisotropies and spectral distortions of the cosmic microwave background (CMB). This stage is followed by a new intermediate phase during which magnetic field energy is mainly converted into kinetic energy of the baryons, building up a turbulent velocity field and producing increasing heating that declines later under turbulent decay. Depending on the PMF strength and spectral index, the onset of turbulent decay can be delayed until $z \simeq 600$, diminishing the expected effects on the CMB anisotropies. We provide several analytic approximations and present numerical results that can be used to study CMB constraints on PMF.

For our investigation, we performed 3D numerical simulations of PMFs along with baryon velocity fluctuations across the cosmological recombination era. Photon drag was included using the standard recombination history obtained with `CosmoRec` and the MHD equations were solved in an expanding medium. Our simulations allow us to trace the flow of energy from the magnetic field, through the baryon velocity field to heating via turbulent decay and dissipation. We are able to describe the net heating rates smoothly across the epoch of recombination enabling a clean separation of real heating, which will lead to an increase of the matter temperature, from drag-dominated energy losses to the CMB photon field, which only leads to secondary temperature perturbations and CMB spectral distortions.

We supported our computations with analytic estimates and provide several useful expressions to represent our numerical results. We find that at redshifts below $z \lesssim 500$, in the regime of well-developed turbulent decay, our new analytic approximation with an additional delay-factor taking the spectral slope into account, gives a slightly better fit.

We observed three main evolutionary stages for magnetic heating: i) an initial phase that is dominated by photon drag ($z \gtrsim 1200$), ii) an intermediate transition period around cosmological

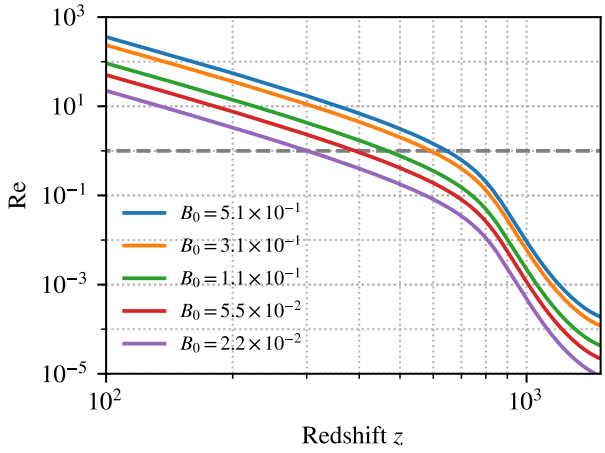

Figure 9: Magnetic Reynolds numbers as a function of redshift for simulation runs where B_0 is varied. The critical magnetic Reynolds number Re = 1 is indicated with a grey dashed line. For different initial amplitudes the Re = 1 redshift varies from $z_{\rm td} \simeq 650$ (fiducial $B_0 = 0.51$) to $z_{\rm td} \simeq 300$. Figure taken from Ref. [74].

recombination, when the photon drag force drops rapidly, and iii) the final fully turbulent MHD phase ($z \lesssim 600$). Only in the latter part of the transition and the turbulent phase do we find significant heating of the medium, a result that is important when deriving and interpreting constraints on PMFs from CMB measurements.

Our computations show that the baryon velocity fluctuations are initially strongly suppressed because of photon drag, but build up during the intermediate transition phase. After recombination, a state approaching equipartition between magnetic and kinetic energy is reached, after which the plasma dissipates energy in a turbulent cascade. In previous treatments, the build-up of the velocity field and its turbulent decay were assumed to proceed instantaneously at recombination ($z \simeq 1100$). Our simulations reveal a substantial delay for the onset of turbulence until redshift $z \simeq 600$–900 (this depends on the amplitude and shape of the initial magnetic power spectrum). In the transition phase, the Lorentz force continuously sources the baryon velocity field until a well developed turbulent state is reached, a process that causes this delay of up to 0.5 Myr.

We also find that the shapes of the net heating rates obtained are broader than previously estimated semi-analytically. Further, for the weaker magnetic fields, their peak broadens to significantly lower redshifts ($z \lesssim 400$). For low magnetic field strengths, the flow reaches turbulence more gradually with the magnetic Reynolds number exceeding unity only in the late stages (see Fig. 9). Steep (blue) spectra produce an earlier peak in the net heating rates at $z_{\rm peak} \simeq 900$. The shape, peak width and epoch of the net heating rate furthermore depends directly on the initial amplitude of the magnetic fields and the spectral index. Our simulations furthermore indicate that the peak magnetic dissipation rate actually occurs once the drag coefficient has already begun to drop sharply and the fluid begins to approach equipartition between magnetic and kinetic dissipation. This again is in contrast to previous interpretations.

Also, while nearly the whole PMF power spectrum is reshaped to a turbulent power-law for the near scale-invariant case, only the intermediate scale wavemodes $k > 10^4$ Mpc^{-1} are

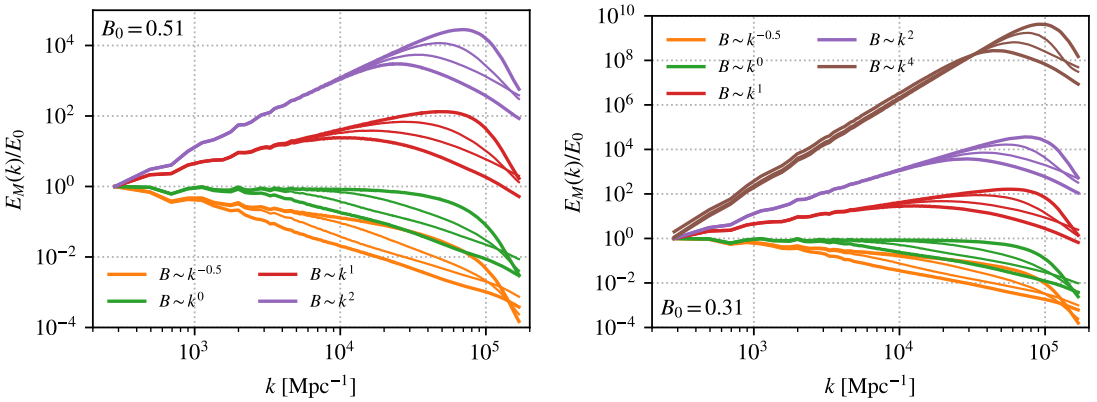

Figure 10: Evolution of the magnetic power spectra of runs with different spectral index n, at four redshifts $z = 2800, 1200, 900$ & 400, decreasing from top to bottom in each panel. The left panel is for $B_{z=3000} = 0.51$ while the right panel shows the curves for $B_{z=3000} = 0.31$. For $B_0 = 0.31$, the case of a causal initial spectrum, $E_M \propto k^4$, is also presented. Figures taken from Ref. [74].

reprocessed for the runs with $E \propto k^1$ and only the smallest scale modes $k > 5.0 \times 10^4$ Mpc^{-1} for the steepest spectrum $E \propto k^4$ (see Fig. 10). The direct observation of the spectral transformation from the initial power-law with cut-off shape to a spectrum in its transitional phase up to the final stage with a turbulent slope is a novel feature of our computations and a benefit of the full 3D treatment of the MHD equations. We can see that for our fiducial case with a near scale-invariant initial power-law with a cutoff at small scales, a turbulent spectrum is developed (with a slope $E \propto k^{-1.4}$ that is slightly shallower than Kolmogorov-type turbulence) as turbulent cascade removes and redistributes power.

To be able to achieve a more complete treatment, more physics at late times need to be included: below a redshift of $z \lesssim 200$ effects like ambipolar diffusion come into play and can contribute substantially to the late time evolution of the magnetic heating history. Stronger magnetic fields along with compressible phenomena would extend the scope of these simulations. A simultaneous treatment of density perturbations induced by PMFs would complement the evolution of heating and its cosmological effects.

References

[1] G. Sigl and N. Leite, *Chiral Magnetic Effect in Protoneutron Stars and Magnetic Field Spectral Evolution*, *JCAP* **1601** (2016) 025, [1507.04983].

[2] R. Alves Batista, A. Dundovic, M. Erdmann, K.-H. Kampert, D. Kuempel, G. Müller et al., *CRPropa 3 - a Public Astrophysical Simulation Framework for Propagating Extraterrestrial Ultra-High Energy Particles*, *JCAP* **1605** (2016) 038, [1603.07142].

[3] L. Merten, J. Becker Tjus, H. Fichtner, B. Eichmann and G. Sigl, *CRPropa 3.1—a low energy extension based on stochastic differential equations*, *JCAP* **1706** (2017) 046, [1704.07484].

[4] S. Hackstein, F. Vazza, M. Brüggen, G. Sigl and A. Dundovic, *Propagation of ultrahigh energy cosmic rays in extragalactic magnetic fields: a view from cosmological simulations*, *Mon. Not. Roy. Astron. Soc.* **462** (2016) 3660–3671, [1607.08872].

[5] R. Alves Batista, M.-S. Shin, J. Devriendt, D. Semikoz and G. Sigl, *Implications of strong intergalactic magnetic fields for ultrahigh-energy cosmic-ray astronomy*, *Phys. Rev.* **D96** (2017) 023010, [1704.05869].

[6] R. Alves Batista and G. Sigl, *Diffusion of cosmic rays at EeV energies in inhomogeneous extragalactic magnetic fields*, *JCAP* **1411** (2014) 031, [1407.6150].

[7] Pierre Auger Collaborations, A. Aab et al., *Observation of a Large-scale Anisotropy in the Arrival Directions of Cosmic Rays above* 8×10^{18} *eV*, *Science* **357** (2017) 1266–1270, [1709.07321].

[8] A. Dundović and G. Sigl, *Anisotropies of Ultra-high Energy Cosmic Rays Dominated by a Single Source in the Presence of Deflections*, 1710.05517.

[9] P. Avola, *On the Role of Liouville Theorem in High Energy Cosmic Ray Anisotropy Studies*, Master's thesis, Universität Hamburg, 2017.

[10] N. Leite, C. Evoli, M. D'Angelo, B. Ciardi, G. Sigl and A. Ferrara, *Do Cosmic Rays Heat the Early Intergalactic Medium?*, *Mon. Not. Roy. Astron. Soc.* **469** (2017) 416–424, [1703.09337].

[11] J. D. Bowman, A. E. E. Rogers, R. A. Monsalve, T. J. Mozdzen and N. Mahesh, *An absorption profile centred at 78 megahertz in the sky-averaged spectrum*, *Nature* **555** (2018) 67–70.

[12] N. Leite, R. Reuben, G. Sigl, M. H. G. Tytgat and M. Vollmann, *Synchrotron Emission from Dark Matter in Galactic Subhalos. A Look into the Smith Cloud*, *JCAP* **1611** (2016) 021, [1606.03515].

[13] J.-E. Schönberg, *Sensitivity of radio emission from galaxy clusters and dwarf spheroidal galaxies to dark matter annihilation*, Master's thesis, Universität Hamburg, 2017.

[14] G. Sigl, *Astrophysical Haloscopes*, *Phys. Rev.* **D96** (2017) 103014, [1708.08908].

[15] M. Schlederer and G. Sigl, *Constraining ALP-photon coupling using galaxy clusters*, *JCAP* **1601** (2016) 038, [1507.02855].

[16] F. P. Huang, K. Kadota, T. Sekiguchi and H. Tashiro, *Radio telescope search for the resonant conversion of cold dark matter axions from the magnetized astrophysical sources*, *Phys. Rev.* **D97** (2018) 123001, [1803.08230].

[17] A. Hook, Y. Kahn, B. R. Safdi and Z. Sun, *Radio Signals from Axion Dark Matter Conversion in Neutron Star Magnetospheres*, 1804.03145.

[18] N. Violante Gomes Leite, *On the Connection Between Particle Physics and Properties of Cosmic Magnetic Fields*, Ph.D. thesis, U. Hamburg, Dept. Phys., 2017. http://ediss.sub.uni-hamburg.de/volltexte/2017/8556/.

[19] M. Schlederer, *Generation of gravitational waves by primordial magnetic fields*, Master's thesis, Universität Hamburg, 2017.

[20] J. M. Wagstaff, R. Banerjee, D. Schleicher and G. Sigl, *Magnetic field amplification by the small-scale dynamo in the early Universe*, *Phys. Rev. D* **89** (May, 2014) 103001, [1304.4723].

[21] R. Beck, *Magnetic Fields in Galaxies*, *Space Science Reviews* **166** (2012) 215–230.

[22] M. L. Bernet, F. Miniati, S. J. Lilly, P. P. Kronberg and M. Dessauges-Zavadsky, *Strong magnetic fields in normal galaxies at high redshift*, *Nature* **454** (2008) 302–304, [0807.3347].

[23] L. Feretti, G. Giovannini, F. Govoni and M. Murgia, *Clusters of galaxies: observational properties of the diffuse radio emission*, *A&AR* **20** (2012) 54, [1205.1919].

[24] Y. Xu, P. P. Kronberg, S. Habib and Q. W. Dufton, *A Faraday Rotation Search for Magnetic Fields in Large-scale Structure*, *AstrophysJ* **637** (2006) 19–26, [arXiv:astro-ph/0509826].

[25] S. Chakraborti, N. Yadav, C. Cardamone and A. Ray, *Radio Detection of Green Peas: Implications for Magnetic Fields in Young Galaxies*, *ApJ* **746** (Feb., 2012) L6, [1110.3312].

[26] A. Neronov and I. Vovk, *Evidence for strong extragalactic magnetic fields from Fermi observations of TeV blazars*, *Science* **328** (2010) 73–75, [1006.3504].

[27] R. Beck, A. Brandenburg, D. Moss, A. Shukurov and D. Sokoloff, *Galactic Magnetism: Recent Developments and Perspectives*, *ARA&A* **34** (1996) 155–206.

[28] D. R. G. Schleicher, R. Banerjee, S. Sur, T. G. Arshakian, R. S. Klessen, R. Beck et al., *Small-scale dynamo action during the formation of the first stars and galaxies. I. The ideal MHD limit*, *Astron. Astrophys.* **522** (2010) A115, [1003.1135].

[29] M. A. Latif, D. R. G. Schleicher, W. Schmidt and J. Niemeyer, *The small scale dynamo and the amplification of magnetic fields in massive primordial haloes*, *Mon. Not. Roy. Astron. Soc.* **432** (2013) 668, [1212.1619].

[30] R. Banerjee, S. Sur, C. Federrath, D. R. Schleicher and R. S. Klessen, *Generation of strong magnetic fields via the small-scale dynamo during the formation of the first stars*, 1202.4536.

[31] J. Schober, D. R. G. Schleicher and R. S. Klessen, *Magnetic field amplification in young galaxies*, *A&A* **560** (Dec., 2013) A87, [1310.0853].

[32] M. S. Turner and L. M. Widrow, *Inflation Produced, Large Scale Magnetic Fields*, *Phys.Rev.* **D37** (1988) 2743.

[33] G. Sigl, A. V. Olinto and K. Jedamzik, *Primordial magnetic fields from cosmological first order phase transitions*, *Phys.Rev.* **D55** (1997) 4582–4590, [astro-ph/9610201].

[34] E. Harrison, *Generation of Magnetic Fields in the Radiation ERA*, *Mon. Not. Roy. Astron. Soc.* **147** (1970) 279.

[35] S. Tsugé, *Approach to the origin of turbulence on the basis of two-point kinetic theory*, *Physics of Fluids* **17** (Jan., 1974) 22–33.

[36] A. Kosowsky, A. Mack and T. Kahniashvili, *Gravitational radiation from cosmological turbulence*, *Phys. Rev. D* **66** (July, 2002) 024030, [astro-ph/0111483].

[37] C. Caprini and R. Durrer, *Gravitational waves from stochastic relativistic sources: Primordial turbulence and magnetic fields*, *Phys. Rev. D* **74** (Sept., 2006) 063521, [astro-ph/0603476].

[38] J. Schober, D. Schleicher, C. Federrath, R. Klessen and R. Banerjee, *Magnetic Field Amplification by Small-Scale Dynamo Action: Dependence on Turbulence Models and Reynolds and Prandtl Numbers*, 1109.4571.

[39] A. A. Schekochihin, S. A. Boldyrev and R. M. Kulsrud, *Spectra and Growth Rates of Fluctuating Magnetic Fields in the Kinematic Dynamo Theory with Large Magnetic Prandtl Numbers*, *ApJ* **567** (Mar., 2002) 828–852, [astro-ph/0103333].

[40] C. Federrath, G. Chabrier, J. Schober, R. Banerjee, R. S. Klessen et al., *Mach Number Dependence of Turbulent Magnetic Field Amplification: Solenoidal versus Compressive Flows*, *Phys.Rev.Lett.* **107** (2011) 114504, [1109.1760].

[41] A. Lewis, *Observable primordial vector modes*, *Phys.Rev.* **D70** (2004) 043518, [astro-ph/0403583].

[42] T. H.-C. Lu, K. Ananda and C. Clarkson, *Vector modes generated by primordial density fluctuations*, *Phys.Rev.* **D77** (2008) 043523, [0709.1619].

[43] T. H.-C. Lu, K. Ananda, C. Clarkson and R. Maartens, *The cosmological background of vector modes*, *JCAP* **0902** (2009) 023, [0812.1349].

[44] A. J. Christopherson, K. A. Malik, D. R. Matravers and K. Nakamura, *Comparing two different formulations of metric cosmological perturbation theory*, *Classical and Quantum Gravity* **28** (Nov., 2011) 225024, [1101.3525].

[45] K. Ichiki, K. Takahashi and N. Sugiyama, *Constraint on the primordial vector mode and its magnetic field generation from seven-year Wilkinson Microwave Anisotropy Probe Observations*, *Phys.Rev.* **D85** (2012) 043009, [1112.4705].

[46] A. Gruzinov, S. C. Cowley and R. Sudan, *Small scale field dynamo*, *Phys.Rev.Lett.* **77** (1996) 4342–4345, [astro-ph/9611194].

[47] R. Banerjee and K. Jedamzik, *The Evolution of cosmic magnetic fields: From the very early universe, to recombination, to the present*, *Phys.Rev.* **D70** (2004) 123003, [astro-ph/0410032].

[48] R. Durrer and A. Neronov, *Cosmological magnetic fields: their generation, evolution and observation*, *A&A Rev.* **21** (June, 2013) 62, [1303.7121].

[49] J. M. Wagstaff and R. Banerjee, *CMB spectral distortions from the decay of causally generated magnetic fields*, *Phys. Rev. D* **92** (Dec., 2015) 123004, [1508.01683].

[50] D. J. Fixsen, E. S. Cheng, J. M. Gales, J. C. Mather, R. A. Shafer and E. L. Wright, *The Cosmic Microwave Background Spectrum from the Full COBE FIRAS Data Set*, *ApJ* **473** (Dec., 1996) 576, [astro-ph/9605054].

[51] A. Kogut, D. J. Fixsen, D. T. Chuss, J. Dotson, E. Dwek, M. Halpern et al., *The Primordial Inflation Explorer (PIXIE): a nulling polarimeter for cosmic microwave background observations*, *JCAP* **7** (July, 2011) 025, [1105.2044].

[52] L. Campanelli, *Evolution of magnetic fields in freely decaying magnetohydrodynamic turbulence*, *Phys. Rev. Lett.* **98** (Jun, 2007) 251302.

[53] L. Campanelli, *Evolution of primordial magnetic fields in mean-field approximation*, *Eur. Phys. J.* **C74** (2014) 2690, [1304.4044].

[54] T. Kahniashvili, A. G. Tevzadze, A. Brandenburg and A. Neronov, *Evolution of primordial magnetic fields from phase transitions*, *Phys. Rev. D* **87** (Apr, 2013) 083007.

[55] A. Brandenburg, T. Kahniashvili and A. G. Tevzadze, *Nonhelical Inverse Transfer of a Decaying Turbulent Magnetic Field*, *Physical Review Letters* **114** (Feb., 2015) 075001, [1404.2238].

[56] Y. Aoki, G. Endrődi, Z. Fodor, S. D. Katz and K. K. Szabó, *The order of the quantum chromodynamics transition predicted by the standard model of particle physics*, *Nature* **443** (Oct., 2006) 675–678, [hep-lat/0611014].

[57] M. Laine and K. Rummukainen, *The MSSM electroweak phase transition on the lattice*, *Nuclear Physics B* **535** (Dec., 1998) 423–457, [hep-lat/9804019].

[58] T. Vachaspati, *Estimate of the Primordial Magnetic Field Helicity*, *Physical Review Letters* **87** (Dec., 2001) 251302, [astro-ph/0101261].

[59] J. M. Wagstaff and R. Banerjee, *Extragalactic magnetic fields unlikely generated at the electroweak phase transition*, *JCAP* **1601** (2016) 002, [1409.4223].

[60] R. Alves Batista, A. Saveliev, G. Sigl and T. Vachaspati, *Probing Intergalactic Magnetic Fields with Simulations of Electromagnetic Cascades*, *Phys. Rev.* **D94** (2016) 083005, [1607.00320].

[61] H. Tashiro, W. Chen, F. Ferrer and T. Vachaspati, *Search for CP violating signature of intergalactic magnetic helicity in the gamma-ray sky*, *MNRAS* **445** (Nov., 2014) L41–L45, [1310.4826].

[62] K. Miyamoto, T. Sekiguchi, H. Tashiro and S. Yokoyama, *CMB distortion anisotropies due to the decay of primordial magnetic fields*, *Phys. Rev. D* **89** (Mar., 2014) 063508, [1310.3886].

[63] J. Ganc and M. S. Sloth, *Probing correlations of early magnetic fields using μ-distortion*, *JCAP* **8** (Aug., 2014) 018, [1404.5957].

[64] J. M. Wagstaff and R. Banerjee, *Extragalactic magnetic fields unlikely generated at the electroweak phase transition*, *JCAP* **1** (Jan., 2016) 002, [1409.4223].

[65] A. Boyarsky, J. Fröhlich and O. Ruchayskiy, *Self-Consistent Evolution of Magnetic Fields and Chiral Asymmetry in the Early Universe*, *Physical Review Letters* **108** (Jan., 2012) 031301, [1109.3350].

[66] A. Boyarsky, J. Fröhlich and O. Ruchayskiy, *Magnetohydrodynamics of chiral relativistic fluids*, *Phys. Rev. D* **92** (Aug., 2015) 043004, [1504.04854].

[67] J. Reppin and R. Banerjee, *Nonhelical turbulence and the inverse transfer of energy: A parameter study*, *Phys. Rev.* **E96** (2017) 053105, [1708.07717].

[68] R. Banerjee and K. Jedamzik, *Evolution of cosmic magnetic fields: From the very early Universe, to recombination, to the present*, *Phys. Rev. D* **70** (Dec., 2004) 123003–+.

[69] C. J. Hogan, *Magnetohydrodynamic effects of a first-order cosmological phase transition*, *Physical Review Letters* **51** (Oct., 1983) 1488–1491.

[70] A. P. Kazantsev, *Enhancement of a Magnetic Field by a Conducting Fluid*, *Soviet Journal of Experimental and Theoretical Physics* **26** (1968) 1031.

[71] D. Biskamp, *Magnetohydrodynamic Turbulence*. Cambridge Univserity Press, 2008, Feb., 2008.

[72] P. Olesen, *Inverse cascades and primordial magnetic fields*, *Physics Letters B* **398** (Feb., 1997) 321–325, [astro-ph/9610154].

[73] L. Campanelli, *On the self-similarity of nonhelical magnetohydrodynamic turbulence*, *Eur. Phys. J.* **C76** (2016) 504, [1511.06797].

[74] P. Trivedi, J. Reppin, J. Chluba and R. Banerjee, *Magnetic heating across the cosmological recombination era: Results from 3D MHD simulations*, *MNRAS* (July, 2018) , [1805.05315].